Long-term trends of NO_y above northern mid-latitudes as inferred from Jungfraujoch, HALOE and ACE-FTS solar observations.

GIRPAS
Groupe InfraRouge de Physique Atmosphérique et Solaire

P. Demoulin[(1)], E. Mahieu[(1)], C. Servais[(1)], B. Lejeune[(1)], W. Bader[(1)], G. Roland[(1)], R. Zander[(1)],
K. Walker[(2)], P. Bernath[(3)], M. Van Roozendael[(4)], F. Hendrick[(4)].

[(1)]*GIRPAS, Institute of Astrophysics and Geophysics, University of Liège, Belgium*
[(2)]*Department of Chemistry, University of Waterloo, Canada & Department of Physics, University of Toronto, Canada*
[(3)]*Old Dominion University, Norfolk, Virginia, USA*
[(4)]*Belgian Institute for Space Aeronomy (BIRA-IASB), Brussels, Belgium*

Université de Liège

INTRODUCTION

The NO_y family of gases, defined as $NO + NO_2 + NO_3 + 2{\times}N_2O_5 + HNO_3 + HNO_4 + ClONO_2 + BrONO_2$, plays an important role in the ozone depletion (NO_x catalytic cycle, Crutzen 1970). At the Jungfraujoch observatory, FTIR spectrometers measure since 1984 the four most abundant members of NO_y i.e. NO, NO_2, HNO_3 and $ClONO_2$. Their sum is a good proxy of NO_y and will be noted here NO_y^* (the most important missing gas being N_2O_5).

FTIR DATA SET

Infrared solar absorption spectra recorded since 1984 at the Jungfraujoch observatory (Swiss Alps, 3580 m a.s.l.):
- 2 FTIR spectrometers (home-made and Bruker 120 HR)
- high resolution (82 to 175 cm max. OPD)
- only clear-sky conditions

ANALYSIS
- total columns
- monthly means (avoid higher weight for period with many observations)
- SFIT 1 and 2
- P, T profiles from NCEP
- spectral micro-windows:
  - NO: 1899.85-1900.20, 1902.92-1903.36 and 1912.70-1912.86 cm^{-1}
  - NO_2: 2914.51-2914.86 cm^{-1}
  - HNO_3: 868.75-869.75 cm^{-1}
  - $ClONO_2$: 779.3-780.6 then 780.050-780.355 cm^{-1}
  - N_2O: 2481.3-2482.6, 2526.4-2528.2, 2537.85-2538.8 and 2540.1-2540.7 cm^{-1}
- NO and NO_2: empirical correction for diurnal variation

TRENDS DERIVATION
- multiple regression model, including a linear trend, a seasonal component and anomalies from various atmospheric parameters (Bodeker *et al*, 1998):
  - solar flux (10.7 cm wavelength, measured at Ottawa / Penticton, Canada)
  - stratospheric aerosol optical depth (15-35 km, 20° N - 50° N) (Vernier *et al*, 2011)
  - tropopause height, calculated from NCEP P,T profiles
  - other investigated parameters: NAO (North Atlantic Oscillation), QBO (Quasi-Biennal Oscillation), pressure, stratospheric temperature
- only statistically significant parameters have been kept

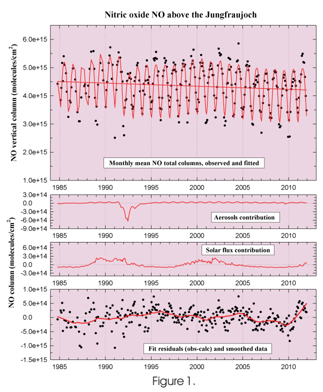

Figure 1.

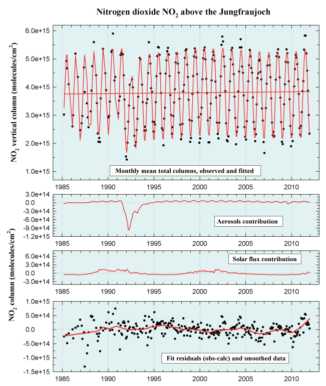

Figure 2.

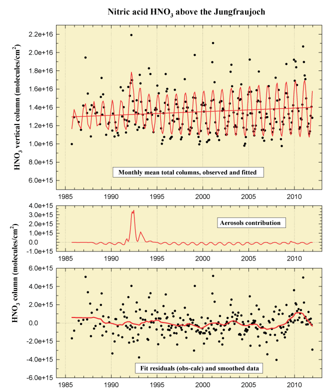

Figure 3.

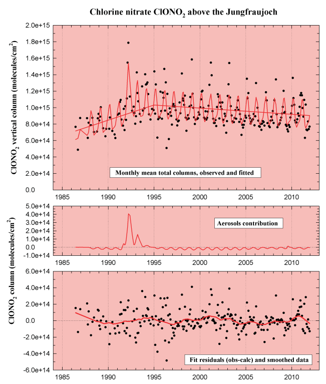

Figure 4.

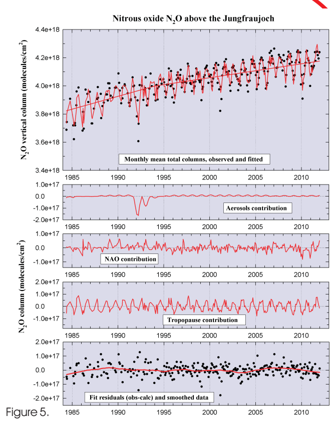

Figure 5.

Figures 1 to 5. Upper frames: monthly mean total columns derived from Jungfraujoch FTIR spectra (black dots), together with best fit of the regression model and linear trends (red lines), respectively for NO, NO_2, HNO_3, $ClONO_2$ and N_2O. For $ClONO_2$, two linear trends have been included in the model, to take into account the decrease of this gas after 1995, as a consequence of the limitation of Cl emissions (Montreal protocol). Two linear trends have also been used for N_2O. Middle frames give the contribution of aerosol optical depth (AOD), solar flux, NAO and tropopause (when applicable) to the total columns. The large aerosol perturbation from the Mt. Pinatubo eruption on June 15, 1991, is clearly visible, sequestering NO_x into HNO_3. The eleven year solar cycle influences NO and NO_2 total columns by a few percents. A summary of these contributions can be found in Table 1.
Lower frames show the residuals of the fit (measured - model) (black dots) together with a smoothed curve (red lines) of these residuals. Note the decrease of NO, NO_2 and HNO_3 during 2006-2007, well visible in the smoothed residuals, as well in Jungfraujoch FTS data and in ACE data.This decrease is followed by an increase in 2008, then by a new decrease in 2009 and again by a large increase in 2010.

gas	NO	NO_2	HNO_3	$ClONO_2$	NO_x	NO_y^*	N_2O	NO/NO_2	NO_y^*/NO_x	N_2O/NO_y^*
seasonal variation (peak-to-peak, %)	45	80	36	38	62	12	4.7	47	61	16
month of the maximum	July	July	February	March	July	April	August	December	January	November
month of the minimum	January	January	August	July	January	October	April	June	August	April
Pinatubo max. contribution (%)	-14	-25	26	44	-37	17	-4.1	28	35	-14
month of maximum	June 1992	April 1992	June 1992	March 1992	June 1992	May 1992	March 1992	Jan. 1992	March 1992	May 1992
solar cycle 22 max. contribution (%)	5.5	3.9	-	-	6.0	-	-	2.9	-	-
month of cycle 22 maximum	June 1989	Febr. 1991			June 1989			Jan. 1989		
solar cycle 23 max. contribution (%)	5.5	3.6	-	-	5.8	-	-	3.0	-	-
month of cycle 23 maximum	Dec. 2001	Dec. 2001			Dec. 2001			Dec. 2001		
NAO contribution (peak-to-peak, %)	-	-	-	-	-	-	3.0	-	-	-
tropopause contribution (p-to-p, %)	-	-	-	-	-	-	3.1	-	-	-

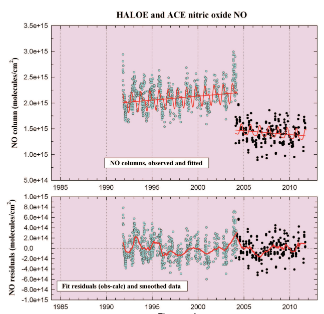

Figure 6.

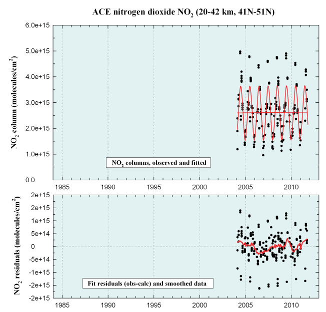

Figure 7.

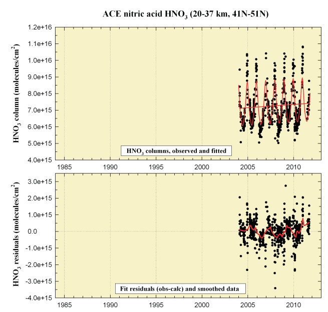

Figure 8.

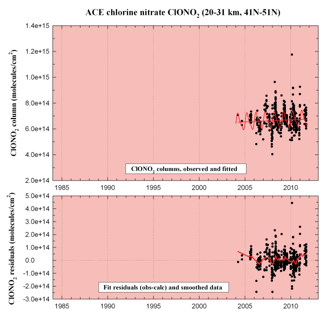

Figure 9.

Figures 6 to 9. Upper frames: partial columns of NO, NO_2, HNO_3, $ClONO_2$ derived from the HALOE (blue dots) and ACE-FTS (black dots) satellite experiments. The red curves correspond to the best fits to the daily means with a linear trend and a 6-term Fourier series, to characterize the long-term changes and seasonal modulations of our target species.
HALOE partial columns have been calculated above 30 mbar pressure level and for latitude belt from 42°N to 52°N. ACE partial columns are for latitude belt from 41°N to 51°N, and for altitude range of 28 - 55 km, 20 - 42 km, 20 - 37 km and 20 - 31 km, respectively for NO, NO_2, HNO_3 and $ClONO_2$.
Lower frames show the residuals of the fit (measured - model) (black dots) together with a smoothed curve (red lines) of these residuals. The minima of NO and NO_2 in 2007 are clearly visible in ACE-FTS data.

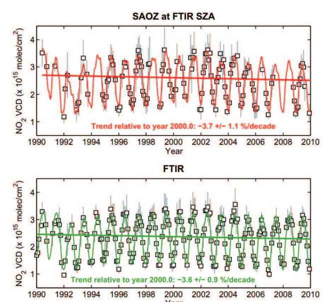

Figure 10.

This figure, from [Hendrick *et al.* 2012], show the NO_2 vertical column time series of 2 co-located NDACC instruments: the ULg FTIR solar spectrometer and the BIRA-IASB SAOZ UV-vis instrument, both operating at the Jungfraujoch observatory. Colored lines correspond to the linear trend (thick line) and to the NO_2 columns recalculated using the multiple linear regression model (thin ligne). Trends derived from both datasets are in very good agreement.

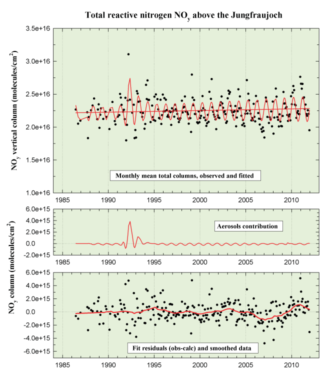

Figure 11.

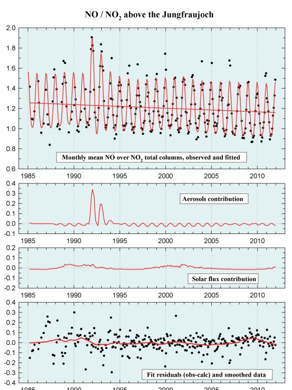

Figure 12.

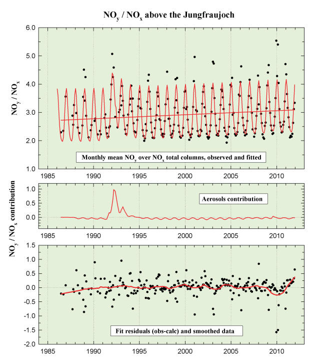

Figure 13.

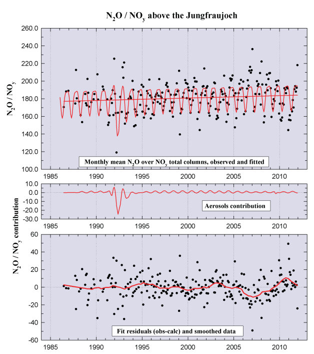

Figure 14.

Figures to 11 to 14: same as Fig. 1 to 5, for NO_y^* and for the ratios NO over NO_2, NO_y^* over NO_x, and N_2O over NO_y^*.
NO_y^* shows no significant trend, but the minimum of 2007-2009 and the increase in 2010 are well marked.
Although N_2O is the source of NO_y^*, NO_y^* is not increasing at the same rate (0.31 ± 0.02 %/year for N_2O, 0.11 ± 0.13 %/year for NO_y^*, see Table 2). This difference is due to increasing CO_2 concentrations cooling the stratosphere (Rosenfield and Douglass, 1998) and to ozone and halogens changes in the stratosphere (McLinden *et al*, 2001).
NO_y^*/NO_x is increasing at a rate of 0.53 ± 0.23 %/year, mainly due to the positive trend of HNO_3, the most abundant NO_y species.
NO/NO_2 is decreasing at a rate of -0.29 ± 0.12 %/year. This decrease is due to increased chlorine loading in the atmosphere, which increases the rate of the reaction [$NO + ClO \rightarrow NO_2 + Cl$]. The increase of NO/NO_2 is expected in the 21st century, as a result of the decreasing chlorine loading and of CO_2-induced stratospheric cooling, which slows the temperature-dependent reaction [$NO + O_3 \rightarrow NO_2 + O_2$] (Revell *et al.*, 2012).

gas	instrum.	begin	end	ref. year	trend (%/yr)	95 % sigma	method
NO	FTS	1984.8	2012.0	1984.0	-0.25	0.12	model & LS
	FTS	1991.8	2004.2	1991.8	0.20	0.28	bootstrap
	HALOE	1991.8	2004.2	1991.8	0.77	0.20	bootstrap
	FTS	2004.1	2011.7	2004.1	-0.73	0.66	bootstrap
	ACE	2004.1	2011.7	2004.1	-0.99	0.83	bootstrap
NO_2	FTS	1985.2	2012.0	1984.0	0.08	0.12	model & LS
	FTS	1990.0	2010.0	1990.0	-0.36	0.09	model & LS
	SAOZ	1990.0	2010.0	1990.0	-0.37	0.11	model & LS
	FTS	2004.1	2011.7	2004.1	0.20	0.57	bootstrap
	ACE	2004.1	2011.7	2004.1	0.14	1.42	bootstrap
HNO_3	FTS	1985.8	2012.0	1984.0	0.31	0.20	model & LS
	FTS	2004.1	2011.7	2004.1	2.08	0.94	bootstrap
	ACE	2004.1	2011.7	2004.1	0.54	0.27	bootstrap
$ClONO_2$	FTS	1986.5	1995.0	1995.0	3.57	1.01	model & LS
	FTS	1995.0	2012.0	1995.0	-0.73	0.34	model & LS
	FTS	2004.2	2011.7	2004.2	0.82	1.07	bootstrap
	ACE	2004.2	2011.7	2004.2	0.50	0.50	bootstrap
NO_x	FTS	1985.1	2012.0	1984.0	0.08	0.16	model & LS
NO_y^*	FTS	1986.5	2012.0	1984.0	0.11	0.13	model & LS
N_2O	FTS	1984.4	1994.0	1994.0	0.46	0.06	model & LS
	FTS	1994.1	2012.0	1994.0	0.25	0.03	model & LS
NO/NO_2	FTS	1985.2	2012.0	1984.0	-0.29	0.12	model & LS
NO_y^*/NO_x	FTS	1986.5	2012.0	1984.0	0.53	0.23	model & LS
N_2O/NO_y^*	FTS	1986.5	2012.0	1984.0	0.16	0.15	model & LS

Table 2. Linear trends retrieved for different gas of the NO_y family and with different instruments. FTS stands for the 2 infrared Fourier transform spectrometers at the Jungfraujoch; SAOZ is the Jungfraujoch UV-visible instrument; HALOE is the space-borne Halogen Occultation Experiment aboard the UARS satellite; ACE is the ACE-FTS instrument aboard the Canadian satellite SCISAT-1.
Trends are given in % per year, relatively to the years indicated in column 5. Column 7 gives the 95 % confidence level of the trends. In column 8, the method used to derive the trends is indicated, either the least squares regression model (for the longer time series) or the bootstrap resampling method (Gardiner et al., 2008).
FTS and SAOZ trends are for total columns. The sensitivity of these techniques to NO_2 is about the same, with no sensitivity in the troposphere and a maximum sensitivity between 20 and 35 km altitude, where the NO_2 concentration in the stratosphere is the largest. NO_2 trends retrieved from these 2 techniques are in perfect agreement.
HALOE trend for NO is for partial columns above 30 mbar pressure level and for latitude belt from 42°N to 52°N. NO trends retrieved from FTS data and from HALOE do not agree, probably because of different altitude sensitivity and range.
ACE trends are for latitude belt from 41°N to 51°N, and for altitude range of 28 - 55 km, 20 - 42 km, 20 - 37 km and 20 - 31 km, respectively for NO, NO_2, HNO_3 and $ClONO_2$. Trends retrieved from FTS and from ACE are in relatively good agreement, except for HNO_3

References

- Bodeker G. E. *et al.*, Trends and variability in vertical ozone and temperature profiles measured by ozone sondes at Lauder, New Zealand: 1986–1996. J. Geophys. Res., 103, 28661–28681, 1998.
- Crutzen P.J., The influence of nitrogen oxides on the atmospheric ozone content, Q.J.R. Meteorol. Soc., 96, 320-325, 1970.
- Gardiner T. *et al.*, Trend analysis of greenhouse gases over Europe measured by a network of ground-based remote FTIR instruments, Atmos. Chem. Phys., 8, 6719-6727, 2008.
- Hendrick F. *et al.*, Analysis of stratospheric NO_2 trends above Jungfraujoch using ground-based UV-visible, FTIR, and satellite nadir observations. Atmos. Chem. Phys. Discuss., 12, 12357-12389, 2012, doi:10.5194/acpd-12-12357-2012.
- McLinden C. A. *et al.,* Understanding trends in stratospheric NO_y and NO_2, J. Geophys. Res.,106(D21), 27 787–27 793, 2001
- Revell L. E. *et al.*, The effectiveness of N_2O in depleting stratospheric ozone. Geophys. Res. Lett., doi:10.1029/2012GL052479, in press.
- Rosenfield J.E. and Douglass A.R., Doubled CO_2 effects on NO_y in a coupled 2D model, Geophys. Res. Lett., 25, 4381-4384, 1998.
- Vernier, J.-P. *et al.*, Major influence of tropical volcanic eruptions on the stratospheric aerosol layer during the last decade, Geophys. Res. Lett., 38, L12807, doi:10.129/2011GL047563, 2011.

Acknowledgements

- Belgian collegues from ULg, ORB/KSB and BIRA-IASB for participation to observation campaigns
- GAW-CH program (MeteoSwiss, Zürich); HFS Jungfraujoch
- A3C and AGACC-II (PRODEX and SSD programs from BELSPO, Brussels)
- the EC NORS project (FP7)
- ACE-FTS team, Canadian Space Agency (CSA) and NSERC, Canada.

Contact: demoulin@astro.ulg.ac.be **http://girpas.astro.ulg.ac.be**